EXPERIMENTAL CALIBRATION OF A ONE-DIMENSIONAL MODEL FOR SIMULATING THE DYNAMIC THERMAL BEHAVIOUR OF STRATIFIED LAKES

Freek Van Riet[1], Ruben De Wolf[1] and Ivan Verhaert [1]

[1]Energy and Materials in Infrastructure and Buildings (EMIB), University of Atwerp, Belgium

ABSTRACT

With increasing insulation, cooling in buildings gains importance regarding overall primary energy consumption. By integrating lakes in cooling systems, this consumption can be reduced. To optimally design these systems, it is beneficial to have insight in the dynamic thermal behaviour of the lake and its interaction with the cooling system. As simulations can provide such insight, a one-dimensional lake model is calibrated and validated in this paper. In order to do so, first the lake's depth was mapped in preliminary measurements. After that, temperature and light intensity at its center were measured at 15 different depths for 11 months. Weather conditions were logged in detail by a national weather station nearby the lake. The preliminary measurements showed that the lake had a maximum depth of $7.8m$, a surface area of $16000m^2$ and a total volume of $100000m^3$. The data of the light intensity showed a time-dependency throughout the year. The calibrated model estimates most data with an error of only $\pm 2^\circ C$. Therefore, it can be used to analyse the potential of the lake for cooling purposes.

INTRODUCTION

Cooling in buildings gains importance regarding overall primary energy consumption. Indeed, higher insulation rates are known to increase the risk for overheating and hence the need for cooling systems in commercial (Chvatal and Corvacho 2009) as well as residential buildings (Verbeke 2017). In this context, surface water can be beneficial by using the water for 'free cooling' or by increasing the COP of chillers. Indeed, it has been applied in practice since decades for both buildings and districts (Jitco 1977; Mitchell and Spitler 2013). At the university of Cornell, e.g., a system is implemented with a SPF of more than 25 (CornellUniverstity 2005). Although surface water cooling remains a niche, the spread of the technology has been encouraged based on some succesfull cost-reducing projects (Newman and Herbert 2009). However, according to Mitchel at al. (Mitchell and Spitler 2013), a major obstacle for this spreading is the absence of design guidelines and tools. Accordingly, it is not surprising that these authors specifically stimulate the readers of their paper for additional experiments.

They also highlight the need for validated lake models to incorporate in simulation-based design tools.

When considering measurements for model validation of surface water, it is important to make a distinction between different types. While, in general, surface water is defined as any water in direct contact with the air, the focus here will be on lakes only. A lake can be characterised by its different thermal layers (stratification). The following terminology is used to describe the layers:

- Epilimnion: the upper layer, which is in direct contact with air, is mixed by the wind which results in a uniform temperature.

- Metalimnion: the middle layer has a temperature gradient. The depth at which this gradient is maximal is called the thermocline.

- Hypolimnion: the lower layer at a constant temperature (theoretically at $4^\circ C$).

Based on the behaviour of these layers throughout the year, Hutchinson and Loffler (Hutchinson and Loffler 1956) classified lakes, of which one type is called 'holomictic'. These are stratified lakes with exception of some periods at which a uniform temperature is present. If only one of such periods occurs in a year, a lake is called 'monomictic'. These lake types require a high spatial resolution of temperature measurements to capture thermal dynamics. Indeed, the size and temperature gradient of the metalimnion will vary over time.

This paper discusses the calibration of a one-dimensional model of a small monomictic lake. First, a one-dimensional model is selected from literature (next section). After that, the experimental set-up will be discussed for both the preliminary experiments and the main experiments. Finally, the estimated model parameters and corresponding simulations are discussed. In the future, this model will be used to assess the benefits of a district cooling system, connected to the lake, at the Science Park of the University of Antwerp, Belgium.

MODEL DESCRIPTION

In general, the physical phenomena of a lake can be separated into two groups: the ones at the surface (across air-water interface) and the ones below the surface.

Air-Water Interface

Thermal phenomena at the surface were documented by Henderson-Seller (Henderson-Sellers 1986):

$$\varphi_{tot} = (1 - A_{sun}) * \varphi_{sun} + (1 - A_{lwi}) * \varphi_{lwi} \tag{1}$$
$$- \varphi_{lwo} - \varphi_{lat} - \varphi_{sen}$$

In this equation, φ's are heat fluxes (W/m^2) and A stands for albedo (dimensionless). Subscripts refer to ingoing short wave radiation (i.e. direct radiation from the sun, *sun*), ingoing long wave radiation (*lwi*), outgoing long wave radiation (*lwo*), latent heat transfer (*lat*) and sensible heat transfer (*sen*). Note that precipitation is neglected as explained in (Henderson-Sellers 1986). In the rest of this paper, φ_{lat} is only used in terms of evaporation, not for freezing. In fact, ice formation is not taken into account at all. The terms of Equation 1 will be discussed hereafter.

For the albedo of the short wave radiation, A_{sun}, a constant value of 0.06 was used in (Douglas and Wrather 1954; Bonnet, Poulin, and Devaux 2000). Also for the albedo of long wave radiation, a constant can be used (0.03, (Henderson-Sellers 1986)). The ingoing and outgoing long wave radiation depends, however, on the ambient temperature T_{amb} and surface temperature T_{sur}, respectively. These relations are given by the Stefan-Boltzmann Law for *grey bodies*:

$$\varphi_{lwo} = \varepsilon_{wat} * \sigma_s * T_{sur}^4 \tag{2}$$

$$\varphi_{lwi} = \varepsilon_{amb} * \sigma_s * T_{amb}^4 \tag{3}$$

in which σ_s is the Stefan-Boltzmann constant ($5.67 * 10^{-8} W/(m^2 * k^4)$) and ε the emissivity ($-$). This latter variable is for a water surface $\varepsilon_{wat} = 0.96$ and for the ambient air $\varepsilon_{amb} = 0.919 * 10^{-5} * T_{amb}^2 * (1 + 0.17 * C^2)$.

C is the degree of cloudiness. The long-wave radiation originates mostly from the water vapour, carbonedioxide and ozon (Douglas and Wrather 1954).

Latent (evaporation) and sensible (convection) heat transfer can be simplified into a single fictitious heat transfer component according to (Henderson-Sellers 1986) using

Sill's method:

$$\varphi_{lat} + \varphi_{sen} = \rho * L_{lat} * E_{lat} \tag{4}$$

with ρ_{wat} the density of water (kg/m^3), L_{lat} the vaporisation enthalpy of water (J/kg) and E_{lat} the evaporation rate (m/s). L_{lat} and E_{lat} can be calculated as:

$$L_{lat} = 1.92 * 10^6 * \frac{T_{wat}}{T_{wat} - 33.91} \tag{5}$$

$$E_{lat} = 1.15 * 10^{-8} * c_D * u^* * (1 + a_3 * c_R) \cdot (e_{sat} - e_{amb}) \tag{6}$$

in which $c_R = \max(0.0017 * (T_{wat} - T_{amb})^{1/3}/(c_D * u^*), 0)$, $a_3 = \min(0.73 * c_R, 1)$, e_{sat} the saturation water pressure (Pa) at $T = T_{wat}$, e_{amb} the vapour pressure of the ambient air (Pa) at $T = T_{amb}$. c_D is the dimensionless dynamical drag coefficient having a mean value of 0.0015 and u^{**} is a fictitious wind velocity (m/s) which can be rewritten in the following equation:

$$u^* = a + b * u \tag{7}$$

in which a and b are parameters to be estimated, and u^* and u the wind velocity at the surface and the measured one above the surface, respectively. These equation takes into account the fact that the wind velocity is not be measured exactly at the surface of the lake. On top of that, by adding the a-parameter, the model allows evaporation at moments wind velocity is measured to be zero.

Below the water surface

Heat transfer under the water surface can be divided in two types:

· Without mass transfer: heat transfer between two adjacent layers by diffusion, and heating by solar radiative heating.

· Coupled to mass transfer: internal streams and turbulences transfer water and thereby heat. The mass transfer is a consequence of wind and internal density differences (buoyancy).

Mass transfer in water is complex and, as a consequence, it requires a high calculation time to be simulated. Therefore, both types of heat transfer (excluding solar heating) are typically described by a fictitious diffusion, called *Eddy diffusion* (Henderson-Sellers, McCormick, and Scavia 1983; Henderson-Sellers 1985). If only vertical heat transfer (i.e. one-dimensional model) and a constant section are assumed, the governing equation can be written as:

$$\frac{\delta T}{\delta t} = \frac{\delta}{\delta z} \left((\alpha + K_H(z)) * \frac{\delta T}{\delta z} \right) + \frac{-\frac{\delta \varphi_{pen}}{\delta z}}{\rho_{wat} * c_p} \tag{8}$$

with t the time (s), z the depth (m) and φ_{pen} the solar radiation in the water (W/m^2). ρ_{wat} and the specific thermal capacity c_p ($J/(kg * K)$) can be calculated according to (Chen and Millero 1986) for a temperature and pressure range of $0 - 30°C$ and $0 - 180 bar$. It can be seen that an extra term $K_H(z)$ is added to the thermal diffusivity α

(m^2/s), compared to Fourier's law. This extra term takes into account the mass transfer-related heat transfer and is called the *Eddy diffusion coefficient*. The two diffusion coefficients can be calculated as:

$$\alpha = \frac{\lambda}{\rho_{wat} * c_p} \tag{9}$$

$$K_H = K_{H0} * f(Ri) \tag{10}$$

with λ the thermal conductivity ($W/(m * K)$). The neutral Eddy diffusion coefficient, K_{H0} (m^2/s), and correction factor for instability of the water $f(Ri)$, can be approximated as:

$$K_{H0} = \frac{\kappa * \overset{*}{w} * z}{P_0} * \exp(-k^* z) \tag{11}$$

$$f(Ri) = (1 + 37 * Ri^2)^{-1} \tag{12}$$

in which κ is the *Von Karman* constant (0.4, dimensionless), P_0 the neutral Prandtl-number ($-$) and k^* ($-$) a parameter characterising the exponential *Ekman* velocity profile (approximated as in (Henderson-Sellers 1985)). The shear velocity $\overset{*}{w}$ (m/s), depends on the wind velocity u^*:

$$\overset{*}{w} = \sqrt{\frac{\rho_{amb}}{\rho_{wat}} * c_D * (u^*)^2} \tag{13}$$

The correction factor $f(Ri)$ depends on the gradient Richardson number Ri. This dimensionless number is a measure for the thermal stability of the water. For the calculation of it, the reader is referred to (Henderson-Sellers 1985). If no stratification is present, Ri will be zero, $f(Ri)$ will be equal to unity and, in turn, K_H will be equal to K_{H0}. Hence, the term 'neutral' that was mentioned before, refers to a situation without stratification.

The solar radiation term from Equation 8, can be described by the Lambert-Beer law:

$$\varphi_{pen} = \varphi_{pen,sur} * \exp(-k_e * z) \tag{14}$$

with $\varphi_{pen,sur}$ the transmitted solar radiation at the water surface (in W/m^2, equal to $(1 - A_{sun}) * \varphi_{sun}$ from Equation 1). k is the light extinction coefficient ($1/m$).

Finally, the heat transfer between water and bottom is neglected in this paper.

Model Parametrisation

In conclusion, the described model is predominantly mechanistic of nature. However, three parameters should be estimated based on measurement data: two parameters for wind and evaporation correction (*a,b*) and one for

characterising the solar penetration (k_e). k_e can be estimated with only measurements of light intensity at different depths, while *a* and *b* require the full model to be ran in an optimisation loop. This was performed with a non-linear least-square solver in Matlab (lsqnonlin).

MEASUREMENTS

Experiments were performed in two steps. In preliminary measurements the three-dimensional shape of the lake was mapped. In the second, loggers were set up in the lake in order to measure the temperature and irradiation at multiple heights.

Preliminary Measurements

A lake at the science park of the University of Antwerp (Belgium) was considered. It is property of POM Antwerpen and has a latitude of $51°06^1$ and a longitude of $4°21^1$. The lake was crossed over with a boat. At multiple positions, the depth of the lake was measured with an acoustic sensor. At the same time, the coordinates were noted using a GPS device. As it was not possible to reach the lake's shore with the boat, extra (coordinate,depth)-pairs of the shore were added to the data set based on satellite images. Obviously, the depths at these positions were set to zero. The dataset allows to map the shape of the lake. Based on this shape, the set-up for the continuous measurements (next subsection) was developed.

Continuous Measurements

In the middle of the lake, 15 loggers were placed to measure temperature and light intensity. The depth of the lake at that postion is 7.5*m*, which means that data was logged each 0.5*m*. This is a double spatial resolution of the measurements compared to (Bonnet, Poulin, and Devaux 2000; Belolipetsky et al. 2010). However, the lakes measured in the latter references were deeper than the one discussed here. Hence it was assumed that a steeper thermocline would be present, requiring that higher spatial resolution.

The experimental set-up is shown in Figure 1. First of all, a buoy connected by a rope to an anchor was placed in the lake. A concrete block was used as anchor. The loggers were fixed perpendicularly to a second rope, also connected to an anchor (brick). By doing so, the loggers could be easily disconnected from the buoy and be read out on the shore. When putting the sensors back in the water after a read-out, a fixed position of measurements could therefore be ensured.

HOBO Pendant Data Loggers were used and were set to save the measured temperature ($°C$) and light intensity (*lux*) at an hourly interval. Light intensity, however, can only be used to measure the relative solar penetration,
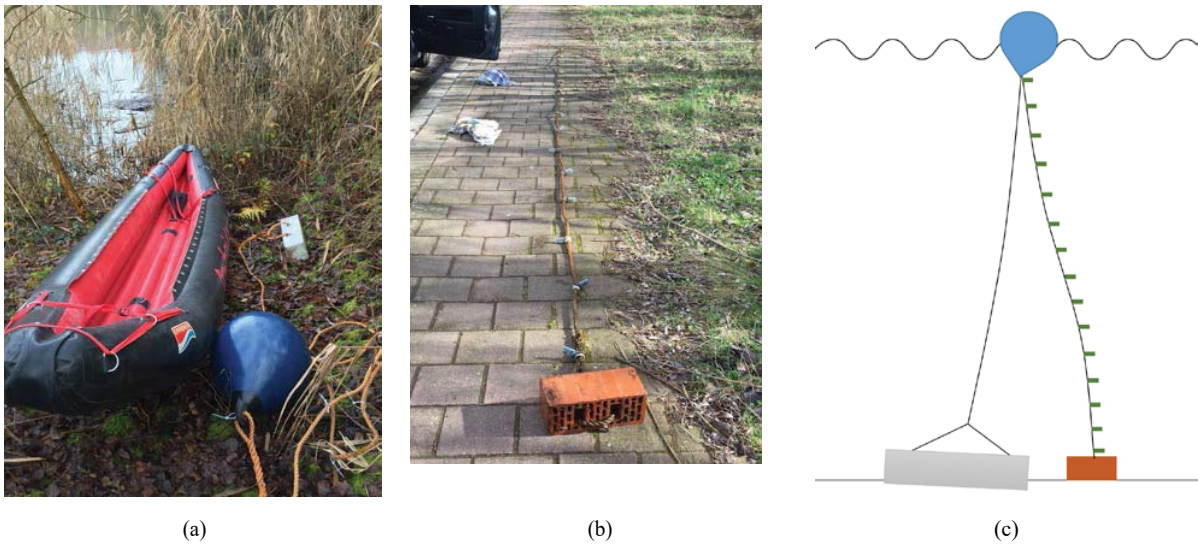
(a)   (b)   (c)

Figure 1: Developed set-up for the performed continuous measurements. First, a fixed anchor with buoy was set in the middle of the lake (a). Then a rope with loggers connected to it was attached to the same buoy (b). Only this latter part of the set-up was disconnected for read-outs. In (c) a schematic overview is given for the complete set-up. Both the fixed anchor and rope with loggers are shown.

rather than absolute intensity. Measurements were started at the 23th of December 2016. While the loggings are still ongoing at the time of writing, for this paper data was used up to the 28th of November 2017 (11 months). The data loggers were read out in 2017 at 16th of February, 21st of March, 8th of May, 14th of July, 22nd of September and 28th of November.

Meteorological data of a nearby weather station was used. The station is located in Sint-Katelijne Waver, at 15 *km* of the lake's location. The following variables were used, as discussed in the section regarding model description: dry bulb temperature, wind velocity, relative humidity, wet bulb temperature, air pressure, solar radiation and the level of cloudiness. The latter variable was measured at another station (Deurne). As justified before, precipitation was neglected.

RESULTS AND DISCUSSION

Size of the Lake

The preliminary measurements are shown in Figure 2. A maximal depth of 7.8m was observed. The total surface area and volume of the lake were found to be 16000m^2 and 100000m^3, respectively. The edges are not exactly vertical, but as a simplification, a constant section was assumed.

Solar Heat Fluxes

First of all, it should be noted that the loggers were found to be covered with algae and chalk at each read-out. As can be seen in the example in Figure 3, this was especially true for the loggers in the upper layers. Before they were put back in the lake they were cleaned. As a consequence, only intensities measured during 48 hours after the moment of read-outs were used to calibrate k_e. It was assumed that in this period algae and chalk build-up could be neglected. During these periods, only the measurements at moments on which at least five sensors measured a light intensity higher than zero were used. Some data of the upper two sensors showed outliers, most likely originating from being overshadowed by the buoy. These observations were removed from the dataset. Finally, k_e-values corresponding to a fit having a R2-value[1] higher than 0.95 were selected.

The results, which can be seen in Figure 4, show a seasonal dependency. Indeed, the extinction coefficient increases up to May. In June, lower values were found, while in September they increased again. The increase towards summer season can be explained by an increased algae population. The decreased values in peak summer (July) might be explained by two factors. First, only few data was withheld for this period. This means that most

---
[1] R2-value were calculated for the upper four metres only. Hence a representative k_e-value for the layers with the highest share of solar heating was ensured.
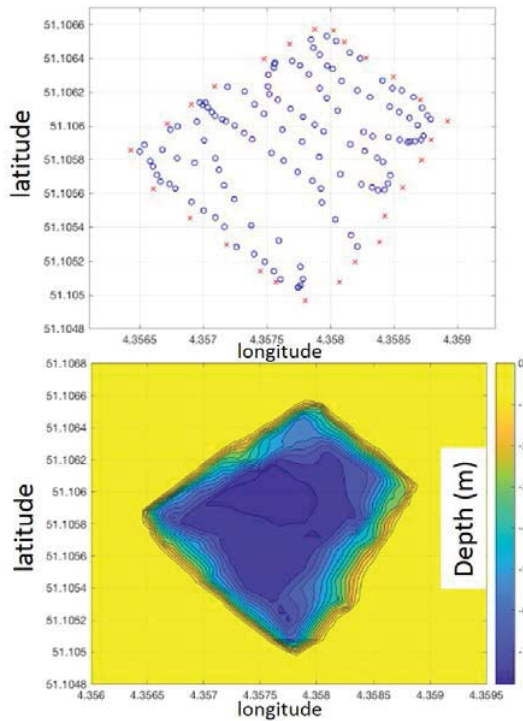
Figure 2: Results of the preliminary measurements. In the upper figure, blue circles refer to measurements with the acoustic sensor, while red crosses indicate added data based on satellite images. The lower figure is a contour plot, showing the estimated depth of the lake.

Figure 3: Example of organic aggregation on the loggers, as observed on the 22nd of September. The upper figure shows the upper sensor, the lower figure shows the second lowest one.
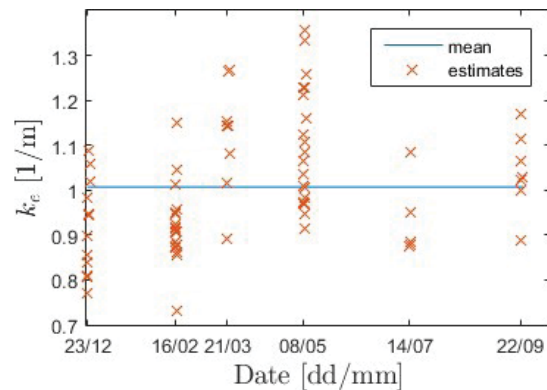
data did not meet the R2-requirement discussed above. Indeed, if a thick layer of algae is present at the very top layer of the lake, the decay of light intensity might not be completely exponential. Other models have been proposed that take into account the absorption in this upper layer (Zaneveld and Spinrad 1980). Second, too high temperature and light intensity might have a negative effect on the growth rate (Bouterfas, Belkoura, and Dauta 2002).

To conclude, precisely quantifying k_e requires to include organic matter growth in the lake model. However, this is outside the scope of this paper. For that reason a constant k_e-value was assumed, equal to $1.0069/m$.

Wind Velocity Correction

The a and b parameters were estimated as $8.74 * 10 - 7m/s$ and 0.226, respectively. Hence, the value found for a suggests that the wind velocity and associated evaporation are neglectable on moments that no wind is measured. However, it should be noted that little moments with a wind velocity close to $0m/s$ were observed in the weather data.

Figure 4: Results of fitted k_e-values for priods after readouts. The mean value is 1.0069. The results show a dependency of the season.

b indicates that the wind velocity above the lake is only 22.6% of the measured one. This makes sense, as the water level of the lake is 3*m* below the ground level and it is surrounded by trees. However, *b* might also compensate for the fixed drag coefficient (see Equation 6 and 13).

Comparison between measurements and simulations

The three parameters discussed above were used to simulate the lake's thermal behaviour. It should be mentioned that the data of the lowest data logger was left out in the analysis, as it showed different dynamics compared to the other data. This might indicate that the sensor was surrounded by mud.

The results and comparison with the measured data can be seen in Figure 5. The measured temperatures clearly confirm that this lake is a monomictic one. In winter, no stratification is present. During spring, an epilimnion is formed, which rises in temperature in summers.

In general, the parametrised model is able to capture the thermal dynamics of the lake: the formation of stratification in spring and the fading out of it in autumn are represented well. In the lowest part of Figure 5, the exact errors can be seen. Most temperatures (96% of the data) are estimated correctly in a range of $\pm 2°C$. In winter, the model underestimated the temperature of the upper layer, though. This might be explained by the fact that no freezing is taken into account. Also, the formation of the epilimnion in spring and further heating up in the beginning of the summer is overestimated more than $2°C$.

CONCLUDING REMARKS

In this paper, a thermal one-dimensional model of a lake was calibrated. Therefore, detailed measurements were performed. In preliminary measurements, the size of the lake was determined. Then, hourly measurements of temperature and light intensity at different layers were performed for 11 months. This data was used to calibrate three parameters of the model: one for quantifying the light extinction and two to compensate for the wind velocity, measured at an other location than the lake itself.

In general, the simulated data is in agreement ($\pm 2°C$) with the measured data. Hence, this model can be used to estimate the potential for cooling at the Science Park. In order to do so, a term should be added to the model to include advection transport (assuming an open loop system is used).

ACKNOWLEDGMENT

REFERENCES

Belolipetsky, Pavel V., Victor M. Belolipetskii, Svetlana N. Genova, and Wolf M. Mooij. 2010. "Numerical modeling of vertical stratification of Lake Shira in summer." *Aquatic Ecology* 44 (3): 561–570.

Bonnet, Marie-Paule, Michel Poulin, and Jean Devaux. 2000. "Numerical modeling of thermal stratification in a lake reservoir. Methodology and case study." *Aquatic Sciences* 62 (2): 105–124.

Bouterfas, Radia, Mouhssine Belkoura, and Alain Dauta. 2002. "Light and temperature effects on the growth rate of three freshwater algae isolated from a eutrophic lake." *Hydrobiologia* 489 (1): 207–217.

Chen, C T A, and F J Millero. 1986. "Precise Thermodynamic Properties For Natural-Waters Covering Only The Limnological Range." *Limnology And Oceanography* 31 (3): 657–662.

Chvatal, Karin Maria Soares, and Helena Corvacho. 2009. "The impact of increasing the building envelope insulation upon the risk of overheating in summer and an increased energy consumption." *Journal of Building Performance Simulation* 2 (4): 267–282.

CornellUniverstity. 2005. How Lake Source Cooling Works.

Douglas, McKay, and W. E. Wrather. 1954. "Water-Loss Investigations: Lake Hefner Studies, Technical Report." *Geological Survey Professional Paper 269*, p. 352.

Henderson-Sellers, B. 1985. "New formulation of eddy diffusion thermocline models." *Applied Mathematical Modelling* 9 (6): 441–446.

Henderson-Sellers, B. 1986. "Calculating the surface energy balance for lake and reservoir modeling: A review." *Journal of Physical Oceanography* 24 (3): 625–649.

Henderson-Sellers, B., M. J. McCormick, and D. Scavia. 1983. "A comparison of the formulation for eddy diffusion in two one-dimensional stratification models." *Applied Mathematical Modelling* 7 (3): 212–215.

Hutchinson, G E, and H. Loffler. 1956. "The thermal stratification of lakes." *Proceedings of the National Academy of Sciences* 42 (2): 84–86.

Jitco, Tracor. 1977. "Feasibility of a district cooling system using natural cold water." *Energy and Environmental systems division* ANL/ICES-T:1–28.

Mitchell, Matt S., and Jeffrey D. Spitler. 2013. "Open-loop direct surface water cooling and surface water heat pump systems-A review." *HVAC and R Research* 19 (2): 125–140.
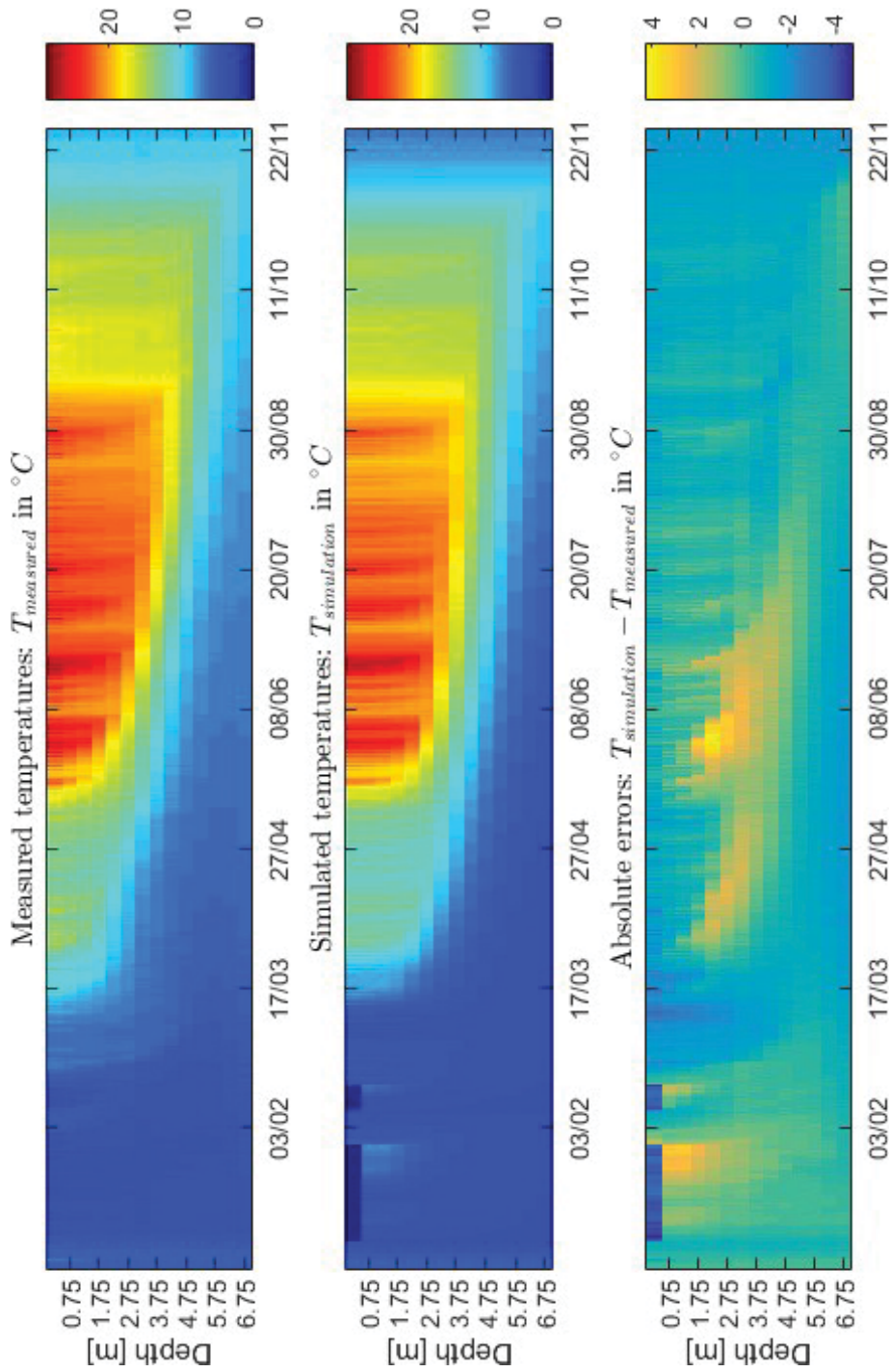
Figure 5: *Comparison between model and data. Upper figure shows the measured temperatures, the middle figure the simulated ones and the lowest the absolute difference between those two (positive values correspond to an overestimation by the model and vice versa). Note that the colors of the upper two figures are identically scaled, while this is not true for the lowest one.*

Newman, Lenore, and Yuill Herbert. 2009. "The use of deep water cooling systems: Two Canadian examples." *Renewable Energy* 34 (3): 727–730.

Verbeke, Stijn. 2017. "Thermal inertia in dwellings: Quantifying the relative effects of building thermal mass on energy use and overheating risk in a temperate climate." PhD, University of Antwerp.

Zaneveld, J Ronald V, and Richard W Spinrad. 1980. "An arc tangent model of irradiance in the sea." 85:4919–4922.

Supscripts

0	at neutral conditions
amb	ambient air
lat	latent
lwi	ingoing long-wave radiation
lwo	outgoing long-wave radiation
pen	penetration into water
sat	saturation
sen	sensible
sun	solar (short-wave) radiation
sur	at surface
wat	water

NOMENCLATURE

Variables

A	albedo: the ratio of reflected radiation and total received radiation of a surface $(-)$
a	correction parameter for wind velocity (m/s)
α	diffusion coefficient (m^2/s)
b	correction parameter for wind velocity $(-)$
C	degree of cloudiness $(-)$
c_D	drag coefficient $(-)$
c_p	the specific thermal capacity $(J/(kg * K))$
e	vapour pressure (Pa)
E_{lat}	evaporation rate (m/s)
ε	emissivity $(-)$
φ	heat flux (W/m^2)
$k*$	a parameter of *Ekman* velocity profile $(-)$
k_e	extiction coefficient $(1/m)$
κ	*Von Karman* constant $(-)$
K_H	eddy diffusion coefficient (m^2/s)
L_{lat}	the vaporisation enthalpy of water (J/kg)
λ	thermal conductivity $(W/(m * K))$
P	Prandtl-number $(-)$
Ri	Richardson number
ρ	density (kg/m^3)
σ_s	Stephan Boltzmann constant $(W/(K^4 * m^2))$
T	absolute temperature (K)
t	time (s)
ϑ	temperature $°C$
u	wind velocity (m/s)
$u*$	corrected wind velocity (m/s)
$\overset{*}{w}$	shear velocity (m/s)
z	depth (m)